

# Investigation of Nd<sup>3+</sup>:YAG Laser Aided Surface Texturing to Improve Tribological Characteristics of Piston Ring

V. Ezhilmaran<sup>1</sup>, L. Vijayaraghavan<sup>1</sup>, and N. J. Vasa<sup>2</sup>

<sup>1</sup>Department of Mechanical Engineering, Indian Institute of Technology Madras, Chennai-600036, INDIA

<sup>2</sup>Department of Engineering Design, Indian Institute of Technology Madras, Chennai-600036, INDIA

E-mail: me13d062@smail.iitm.ac.in

Laser surface processing is increasingly used to improve the tribological properties of sliding surfaces over the last few decades. Texturing in the form of dimples which are evenly spaced helps to reduce friction to a greater extent. But optimizing the size of the dimples with appropriate area density and aspect ratio is a big challenge for the tribologist. This paper aims at the investigation of producing textured surface using nanosecond pulsed Nd<sup>3+</sup>: YAG laser on the surface of piston rings and also to study its frictional properties using a reciprocating tribometer. Experimental analysis on the effect of diameter area density and aspect ratio of the dimples has been demonstrated to improve frictional performance under different lubrication regimes. Friction tests were carried out with both non-textured and textured piston rings by varying the normal load applied on it using synthetic oil as a lubricant at an oil bath temperature of 180°C. A maximum frictional reduction of up to 69% was observed with the nanosecond pulsed laser textured sample at high loading conditions. But nanosecond pulsed laser texturing is always accompanied by recast layer, heat affected zone and micro cracks which may affect the surface properties and in turn the frictional properties of sliding surfaces. Preliminary studies on surface texturing was performed using a femtosecond pulsed laser to improve the surface morphology and tribology characteristics of a piston ring surface.

DOI: 10.2961/jlmn.2017.03.0004

**Key words:** texturing, piston ring, liner, laser, automotive, friction, tribology

## 1. Introduction

Investigation of friction between the lubricated piston rings especially compression ring and cylinder liner wall has attracted many researchers in the current scenario. It is due to the need of improving the efficiency of the internal combustion engines by maintaining a thin oil film under the different lubricating regimes, such as boundary, mixed and hydrodynamic. As the engine is operating with varying speed and load in all the four strokes, the film thickness changes dynamically. During compression and power strokes, the normal load acting on the piston rings are very high, leading to very high friction and wear. The engine works in boundary lubrication regime, during the initial period of the compression stroke and combustion stroke, which in turn leads to high friction and wear. The lubricating regime is mixed between the top dead center and mid-stroke and also between mid-stroke and bottom dead center usually at high loading condition. Hence all the texturing related research in piston rings and cylinder liner aims at minimizing frictional force in these two stages which is quite challenging.

Surface irregularities, such as texture on the sliding surface play a prominent role in influencing the tribological performance of the engine. Surface texturing increases the local hydrodynamic pressures by increasing the oil film thickness in the clearance between the piston ring and cylinder [1]. It was also reported that a friction reduction of up to 38% can be achieved in textured surface compared to the smooth surface [1]. Etsion et al. [2] performed laser surface texturing on piston rings using Nd<sup>3+</sup>:YAG laser with a power of 11 kW, pulse duration of 30 ns, pulse

repetition rate of 5 kHz and energy of 4 mJ/pulse. Laser surface texturing of piston rings increased the lubricant thickness and thereby reducing friction [2]. The dimples help to reduce friction by providing hydrodynamic lift, acts as a reservoir of engine oil and as a micro-hydrodynamic bearing [3]. A thin oil film always exists between the sliding surfaces that are textured and therefore a certain amount of oil is always stored in each dimple. When the thin oil film is broken during boundary lubrication regime, oil in each dimple flows out spontaneously to lubricate the surface by virtue of the free energy reduction [4].

To realize the benefit of surface texturing an appropriate selection of geometrical parameters suitable for particular tribological application is essential. This includes the aspect ratio and area density of the dimples with suitable dimple size [5]. Yali Zhang et al. [6] recommended the dimple diameter of 60 μm, depth of 12 μm for creating a texture surfaces on barrel shaped rings. Based on the modeling results, it has been found that a dimple diameter and depth of 80 μm and 12 μm was beneficial for the textured surface [7]. In the case of piston rings, a dimple diameter of 100 μm was recommended to achieve the beneficial effect of texturing [8]. Previous studies showed that the aspect ratio was also an important parameter for the dimples to build up the hydrodynamic pressure and to reduce friction [9]. Dimple depth should be of sufficient size to get the complete hydrodynamic effect. High depth of the dimples may not create the required hydrodynamic effect in all the tribological conditions like speeds, loads, and viscosities of the oil. Dimples with very low depth

neither increase the hydrodynamic effect nor store the oil. Hence, a careful selection of depth of the dimple for the selected dimple diameter is a big challenge for the tribologist. Another important parameter that influences friction is dimple area density. When the dimple area density is high, the dimples are very close to each other, so the film pressure developed in one dimple can be suppressed by the cavitation effect in the next dimple [10]. With the increase of pitch between the dimples, such negative action can be avoided. But at the same time, low dimple area density is also not recommended for any tribological applications, as less number of dimples cannot produce enough hydrodynamic lift [11]. Wakuda et al. [12] recommended dimple area density of 5–20% for the sliding surfaces to perform better under different lubricating regimes. Zhou et al. [13] concluded that the load carrying capacity varies with dimple area density and dimple depth over diameter ratios and the beneficial effect of texturing was obtained only at high speeds. The depth to diameter ratio of 0.1 was considered to be optimum for the dimple diameters ranging from 252  $\mu\text{m}$  to 564  $\mu\text{m}$  under any operating conditions. On the other hand, Kim et al [14] fabricated the textured surface with two different dimple aspect ratios of 0.14 and 0.3 for each of the dimple diameters, such as 80  $\mu\text{m}$ , 106  $\mu\text{m}$  and 130  $\mu\text{m}$  on the cast iron disk.

Tang et al. [15] conducted a sliding test for 7 hours between textured medium carbon steel sample and high alloy steel counter sample using reciprocating tribometer. Their work concluded that the wear amount of the 5% dimple area fraction sample is approximately 72% less than that of the non-textured sample. Daniel Braun et al. [16] conducted tribology test using a pin on disk for the speeds ranging from 2000 mm/s to 40 mm/s. The entire tribology test for the range of speeds was completed in 300 seconds and the behavior of the textured surface was predicted with in few cycles of the test.

In this study, nanosecond pulsed Nd<sup>3+</sup>:YAG laser with a wavelength of 532 nm was used to produce texture surfaces on chromium coated piston rings. The influence of texture parameters, such as dimple area density and aspect ratio of different dimple diameters were experimentally verified using reciprocating tribometer. All the samples were tested for coefficient of friction in a stepwise increase of load from low to high to identify various lubricating regimes. In order to verify the influence of thermal effects on friction and wear, a ring sample was textured by using femtosecond pulsed laser. Friction results were then compared between the samples textured by using both nanosecond and femtosecond pulsed lasers. A comparative study of wear on the liner surface tested with the non-textured and textured ring samples was performed.

## 2. Experimental details

### 2.1 Laser surface texturing and characterization

A Q-switched, nanosecond pulsed Nd<sup>3+</sup>:YAG laser (Quantel, Brilliant B) providing Gaussian pulse (TEM 00) with a maximum average power of 3.25 W at a wavelength of 532 nm, pulse duration of 6 ns (full width at half maximum) and a pulse repetition rate of 10 Hz was used to produce micro-dimples (Fig. 1). The texture in the form of evenly distributed circular dimples was generated on the

moly-chrome material (94% Cr, 5.5% O, 0.2% Al 0.2% Mo and 0.1% B) coated on the surface of the piston ring. The coating thickness of moly-chrome was measured to be 130  $\mu\text{m}$ . The hardness of the moly-chrome coating was measured to be 941 HV. For the ease of handling, segmented piston ring of radial length 17 mm was used. After establishing a clear relationship between the Nd<sup>3+</sup>:YAG laser parameters and dimple geometry, such as the depth and diameter [19], textured surfaces were produced on the surface of the piston ring. The laser beam was focused using plano-convex lenses with focal lengths of 100 mm, 200 mm and 500 mm to produce dimples of desired diameters, such as 40  $\mu\text{m}$ , 80  $\mu\text{m}$  and 130  $\mu\text{m}$ . Desired dimple parameters were obtained also by controlling the laser pulse energy and number of pulses. The spot diameter was assumed to be the same as that of dimple diameter. The values of laser energies used to produce dimples with the diameter of 40  $\mu\text{m}$ , 80  $\mu\text{m}$  and 130  $\mu\text{m}$  were 8, 15 and 20 mJ, respectively. All the samples were textured in the air ambience. Texture parameters, such as dimple area density, aspect ratio for different dimple size were considered in the analysis. A total of twelve textured samples were fabricated as shown in Table 1. Textured samples with different dimple area densities, such as 5%, 16%, 27% and 38% were fabricated for each dimple size. The dimple aspect ratio of 0.3 was initially considered for the analysis. Number of laser pulses essential to achieve required aspect ratio of 0.3, were 12, 16 and 20, respectively. The selection of dimple aspect ratio of 0.3 was based on the previous studies [14]. Moreover, the initial aim was to find the influence of dimple area density. So, choosing a high dimple aspect ratio of 0.3 was essential to clearly distinguish the influence of other dimple parameters, such as dimple diameter and dimple area density.

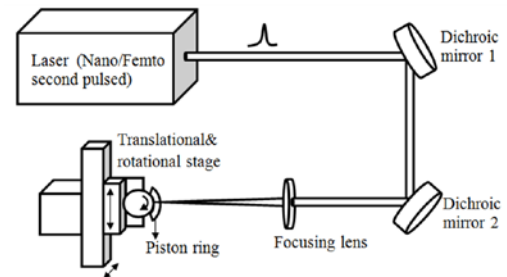


Fig. 1. Laser texturing set up.

The textured parameter which showed minimum friction among the twelve tested samples was chosen to find the influence of aspect ratio. The area density is expressed as  $A_d = (A_t/A_p \times 100\%)$ , where  $A_d$  is the dimple area density,  $A_t$  is the total area occupied by dimples and  $A_p$  is the total area of the piston ring surface. Aspect ratio is given by  $a = (d/D)$ , where  $a$  is the aspect ratio,  $d$  is the dimple depth and  $D$  is the dimple diameter.

Also, femtosecond pulsed laser texturing was carried out on a piston ring sample. A femtosecond pulsed Ti<sup>3+</sup>:Sapphire laser (Coherent, Astrella) with a maximum average power of 5.14 W, center wavelength of 800 nm, pulse repetition rate of 1 kHz, pulse width of approximately 120 fs was used to produce dimples on the piston ring

surface. The depth and diameter of dimples formed were recorded by using a confocal microscope (Olympus LEXT, OLS 4000 model). The roughness of the liner sample was measured and analyzed by using a 3D non-contact surface profiler (Bruker, Contour GT). The surface morphology of the textured surface was obtained by using a scanning electron microscope (FEI, Quanta 200).

**2.2 Friction testing procedure**

The friction testing was carried out using reciprocating type friction testing tribometer (Ducom TR-285-M9 model) (see Fig. 2). The tribometer system consists of moving piston ring sample loaded against the cylinder liner. The material used for the liner was grey cast iron of hardness 380 HV. The piston ring was carefully fixed in the holder attached to the connecting rod arm of the reciprocating tribometer. Then the piston ring was gently placed over the segmented portion of the cylinder liners. 20W-50 synthetic oil was poured onto the liner until the liner track was completely drowned inside the oil. The oil bath was heated to a stabilized oil temperature of 180°C in order to resemble the effect of real engine conditions.

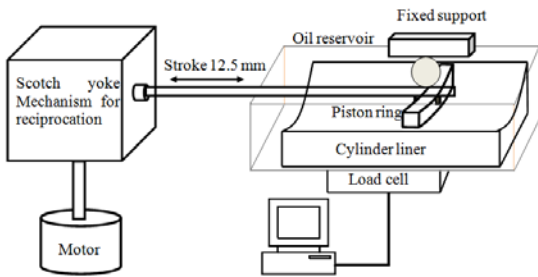


Fig. 2 Reciprocating type friction testing tribometer.

The machine was equipped with a piezoelectric load cell for measuring friction force. The temperature of the oil was monitored continuously by using resistance temperature detector. The stroke length of the piston ring was set at 10 mm and the engine speed was set at 600 rpm. As the tribometer was reciprocating type, the sliding speed varied as a function of crank angle. The rotational motion of the motor was changed into reciprocating movement by a scotch yoke mechanism. The tribology test was carried out with the textured ring samples of various dimple parameters shown in Table 1. To distinguish various lubricating regimes, the test was carried out in a stepwise increase of load from low to high, each for a period of 600 seconds. Average friction coefficient was then calculated on the basis of average values taken from each of the loads for all the samples. The test was repeated multiple times ensure the reliability of the results. The entire friction test was carried out as per ASTM G181-11 standard.

**3. Sample preparation**

In the case of nanosecond pulsed laser, re-deposition layer which is formed around the circumference of the dimples due to high melt flow should be removed by post-processing, to get the full benefits of surface texturing [17]. This is due to the fact that re-deposition reduces the effective lubricant film thickness in the vicinity of the dimple [18]. Figure 3(a) shows the SEM image of a textured surface and the corresponding 3D profile of the

single dimple (Fig. 3(b)). The surface profiler image shows that the debris in the form of recast layer were formed around the dimple circumference after laser texturing (Fig. 4(a)). The debris generated during laser texturing was carefully polished away by using diamond paste of size 3 μm. Figure 4(b) shows the morphology of the textured surface after 10 minutes of polishing. To completely

**Table 1** Various dimple parameters of textured piston rings surface to find the influence of area density.

Piston rings texture parameters (Sliding surface)		
Dimple diameter $D$ (μm)	Area density $A_d$	Aspect ratio $a$
40	5%	0.3
40	16%	0.3
40	27%	0.3
40	38%	0.3
80	5%	0.3
80	16%	0.3
80	27%	0.3
80	38%	0.3
130	5%	0.3
130	16%	0.3
130	27%	0.3
130	38%	0.3
Non-textured		

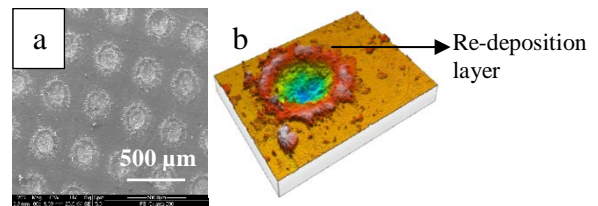


Fig. 3 (a) SEM image of the nano-second pulsed laser textured sample ( $D = 130 \mu\text{m}$  and  $A_d = 16\%$  and  $a = 0.2$ ) and (b) surface profiler image of single dimple.

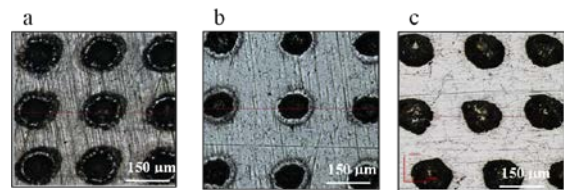


Fig. 4 Surface morphology of the dimple ( $D = 130 \mu\text{m}$  and  $A_d = 16\%$  and  $a = 0.2$ ) (a) After texturing, (b) After diamond polishing (for 10 minutes) and (c) After diamond polishing (for 20 minutes).

remove the re-deposition layer around the dimple circumference, the polishing operation was carried out further for a period of 10 minutes. Figure 4(c) shows that the textured surface was clean and debris free. Then, ultrasonic cleaning was performed in an acetone bath for a period of 20 minutes prior to all tribological tests to remove the debris that was present inside the dimple.

4. Results and discussion

4.1 Influence of area density

As the reciprocating type tribometer was used to find the coefficient of friction, a clear distinction of various lubricating regimes is essential. The lubricating regime more often changes because of change in speed and loading conditions. To distinguish various lubricating regimes, all the textured samples were tested at different loads, such as 10 N, 50 N, 90 N and 130 N and the results were compared with the non-textured sample. The nominal contact pressures at various loads, such as 10 N, 50 N, 90 N and 130 N were estimated as 0.7 MPa, 3.7 MPa, 6.8 MPa and 9.5 MPa, respectively. The textured ring samples of various dimple area densities for the each dimple size of 40 μm, 80 μm and 130 μm is shown in Figs. 5(a-c). Samples with different dimple area densities, such as 5%, 16%, 27% and 38% were fabricated. The corresponding profile of the dimples for the different dimple sizes is shown in Figs. 5(d-f). A slight mismatch in the dimple orientation was attributed to the imprecision in the semi-automatic rotary drive. The dimple orientation effect on friction is mainly based on the contact pair. Previous studies have experimentally described the influence of dimple orientation angle on friction for conformal contact condition using a pin on disk apparatus [20]. But in the case of barrel shaped piston rings, the literature on the influence of dimple orientation effect was not found. Moreover, the contact between the ring and the liner was not fully conformal. Hence, the dimple orientation effect on wear was not considered in the experimental analysis.

Figure 6 shows the typical coefficient of friction graph for the non-textured and textured ring sample of dimple diameter 130 μm. Influence of dimple area density and tribometer loading condition on friction was examined in the test. A dynamic variation of friction for the non-textured sample at a load of 130 N indicated the influence of wear debris on friction. Figures 7(a) to (c) shows the average coefficient of friction as a function of normal load for the non-textured and textured surfaces of different dimple diameters. The average coefficient of friction for the dimple diameter of 40 μm is shown in Fig. 7(a). Less friction was observed when the tribology test was carried out initially at a lesser load of 10 N for all the samples. Asperity contact during initial loading conditions influence the friction values at a lesser load of 10 N. A slight dip in friction value was observed, when the loading was increased from 10 N to 50 N. Asperities removal and behavioral change of the samples to function as a source of

hydrodynamic pressure generation is the main reason for friction reduction at a load of 50 N. The friction coefficient increased with the further increase of load (90 N) and reached a maximum value at a high load of 130 N. Most of the textured samples showed a minimum friction at almost all the loading conditions compared to non-textured sample. The textured sample with dimple area density of 5% and 38% showed high friction compared to the non-textured sample at all the loads. The quantity of the lubricant stored by the dimple of size 40 μm with  $A_d$  of 5% is less. Hence,

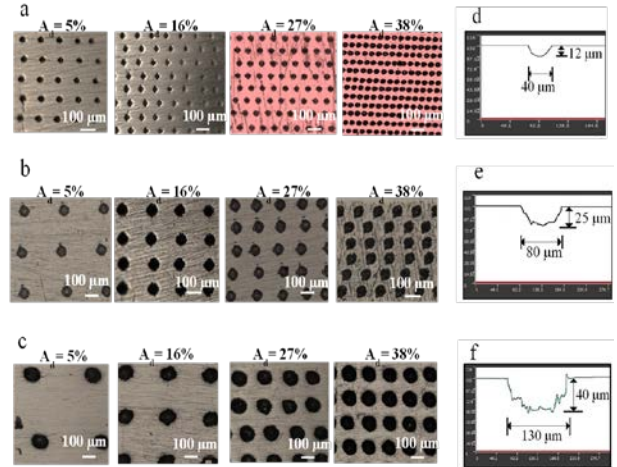


Fig. 5 Confocal microscopic images showing dimple diameter of (a)  $D = 40 \mu\text{m}$ , (b)  $D = 80 \mu\text{m}$ , (c)  $D = 130 \mu\text{m}$  and the corresponding profile of the samples with dimple depth of (d)  $d_d = 12 \mu\text{m}$ , (e)  $d_d = 25 \mu\text{m}$ , (f)  $d_d = 40 \mu\text{m}$ . All samples were maintained at an aspect ratio  $a = 0.3$ .  $A_d$ : Dimple area density varying from 5% to 38%.

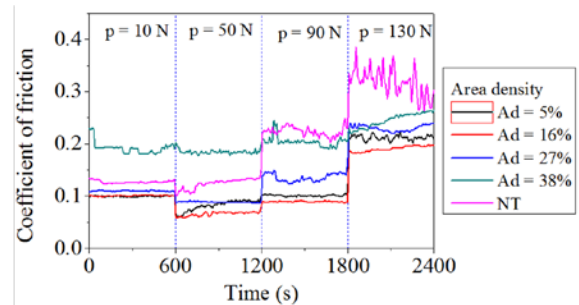


Fig. 6 Typical coefficient of friction graph as a function of time for non-textured and textured samples of different dimple area density for the stepwise increase of load ( $D = 130 \mu\text{m}$  and  $a = 0.3$  for all the samples). NT: Non-textured sample.

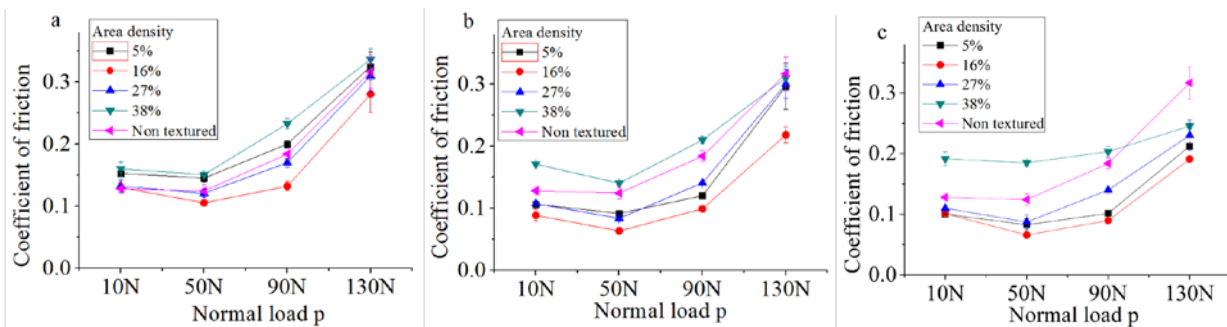


Fig. 7 Average coefficient of friction as a function of normal load corresponding to different values of area density for the dimple diameter of (a) 40 μm, (b) 80 μm and (c) 130 μm.

the friction was high with the textured sample with  $A_d = 5\%$ . The highest friction coefficient was observed in a textured sample with dimple area density of 38%. Though a large number of dimples ( $A_d = 38\%$ ) present to store the lubricant, the non-availability of lubricant at the non-dimple surface might be the reason for high friction. Remaining dimple area densities of 16% and 27% showed minimum friction compared to the non-textured sample at all the loading conditions. In the case of textured surface with less and moderate dimple area densities ( $A_d = 16\%$  and 27%), the probability for the lubricant to immediately enter the next dimple is less. So, the lubricant after coming out of the dimple can freely lubricate the surface to minimize friction.

Figure 7(b) shows the coefficient of friction graph for the non-textured and textured samples for the dimple diameter of 80  $\mu\text{m}$ . The dimple area densities and loading conditions were maintained at same values as that of the dimple diameter of 40  $\mu\text{m}$ . The results showed a decrease in friction compared to the dimple diameter of 40  $\mu\text{m}$  at loads of 10 N, 50 N and 90 N, respectively. But at a high load of 130 N, almost all the friction values of the textured samples remain unaltered. Dimple area density of 16% showed an overall minimum friction at almost all the loads. The overall friction of the textured sample with dimple area density of 27% was more than that of dimple area density of 5% and 16%. Textured sample with dimple area density of 38% showed the highest friction compared to the remaining samples.

When the dimple diameter was increased to 130  $\mu\text{m}$ , the coefficient of friction for all the textured samples reduced phenomenally at a load of 90 N and 130 N (Fig. 7(c)). The lowest friction was observed in the textured sample with dimple area density of 16%. The value of coefficient of friction corresponding to the dimple area of density of 5% and 27% was found to be slightly higher than that of when the dimple area density was 16%. The value of coefficient of friction was even higher for the textured sample with dimple area density of 38%. But at a load of 130 N, friction was comparatively lesser in the textured sample with  $A_d = 38\%$  than the non-textured sample. To summarize, the textured samples having larger dimple size ( $D = 130 \mu\text{m}$ ) showed a significant reduction in friction, especially at a high load of 130 N. The overall results concluded that the beneficial effect of texturing was obtained by selecting suitable dimple parameters.

#### 4.2 Lubricating regimes

The various lubricating regimes of the relatively sliding surfaces can be identified by Stribeck curve. The Stribeck curve which shows various lubricating regimes is shown in Fig. 8. The Stribeck curve is drawn between the coefficient of friction and the lubricating parameter which is given by  $\eta V/p$ , where  $\eta$  is the lubricant viscosity,  $V$  is the sliding velocity,  $p$  is the applied load. As the sliding velocity changes with respect to the crank angle, the lubricating regime is expected to vary often at each position of the sliding surface. The velocity reaches zero at the dead centres and maximum at the mid stroke. Hence, for all the ring samples, the lubricating parameter is zero at the dead centers and maximum at the mid stroke.

Figure 8 shows, a Stribeck curve depicting various lubricating regimes for the dimple diameter of 130  $\mu\text{m}$  having an aspect ratio of 0.3. The Stribeck curve was plotted based on the lubricating parameter and the corresponding value of the average coefficient of friction. The lubricant viscosity (0.004 N-s/m<sup>2</sup>) and the loading condition (50 N) were considered for plotting the Stribeck curve. Irrespective of varying texture parameters, boundary lubrication occurs at the dead centers for all the samples. When the ring travels between the dead centers and mid-stroke positions, linear velocity slowly increases. Hence the lubricating regimes slowly changed from boundary to mixed. When the ring attains a maximum speed at the mid-stroke position, a thin film of lubricant exists to lubricate the surface and the lubrication regime shifted to hydrodynamic. The duration of hydrodynamic lubrication depends upon the suitable texture parameters chosen for the study. In the present case, the values of coefficient of friction were low for the dimple area densities of 5, 16 and 27%. So, it is presumed that predominantly mixed and hydrodynamic lubrication occurred during the entire stroke. Whereas with the non-textured and textured sample with  $A_d = 38\%$  the friction was comparatively higher. So, mostly boundary and mixed lubrication occurred in these samples during the entire stroke.

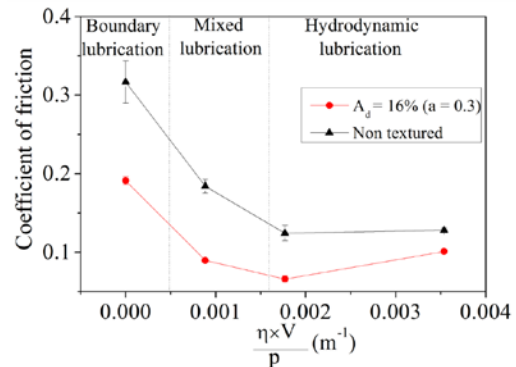


Fig. 8 Schematic of Stribeck curve for various lubricating regimes ( $D = 130 \mu\text{m}$  and  $p = 50 \text{ N}$ ).

#### 4.3 Influence of aspect ratio

In order to find the influence of dimple aspect ratio, three different piston ring samples with dimple aspect ratios, such as 0.1, 0.2 and 0.3 were textured by using nanosecond pulsed laser as shown in Figs. 9(a-c). Figures 9(d) to (f) shows the corresponding dimple profiles. Dimple diameter of 130  $\mu\text{m}$  and dimple area density of 16% was maintained in all the samples (Table 2). The laser pulse energy used to produce the dimple of desired size was 20 mJ. Number of laser pulses essential to achieve required aspect ratios of 0.1, 0.2 and 0.3 were 8, 14 and 20, respectively. Based on the tribology study, as shown in Fig. 10, a clear distinction of textured samples in terms of friction coefficient was observed at a high load of 130 N. The dynamic variation in friction coefficient was not observed even at a high load of 130 N. This verified the existence of a thin film between the relatively sliding surfaces. Based on the Fig. 11, the textured samples showed less friction compared to non-textured samples at all the loading conditions. The lowest friction was noticed

in the textured sample with dimple aspect ratio of 0.2 followed by 0.1. Among the textured samples, a high friction was noticed in the sample with dimple aspect ratio of 0.3. This revealed that a suitable dimple depth corresponding to the dimple diameter is essential to realize the beneficial effect of texturing. The generation of hydrodynamic effect might be less with less dimple aspect ratio ( $A_d = 0.1$ ), whereas the generation of hydrodynamic

**Table 2** Various dimple parameters to find the influence of aspect ratio.

Dimple diameter $D$ ( $\mu\text{m}$ )	Area density $A_d$ %	Aspect ratio $a$
130	16%	0.1
130	16%	0.2
130	16%	0.3

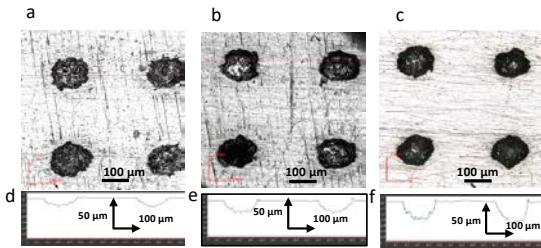


Fig. 9 Confocal microscopic images showing different dimple aspect ratio of (a) 0.1, (b) 0.2 and (c) 0.3 ( $D = 130 \mu\text{m}$ ,  $A_d = 16\%$  for all the samples).

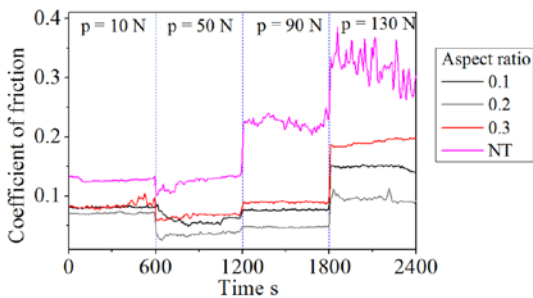


Fig. 10 Typical coefficient of friction graph obtained from the tribology test showing the influence of different dimple aspect ratio for the stepwise increase of load ( $D = 130 \mu\text{m}$  and  $A_d = 16\%$  for all the samples).

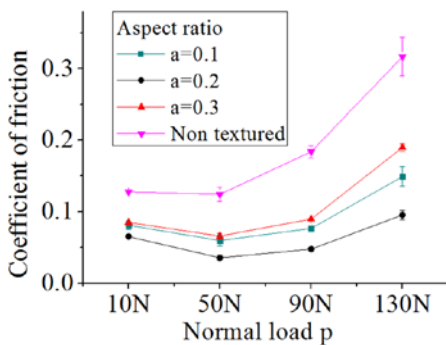


Fig. 11 Average coefficient of friction as a function of load for the non-textured and textured samples of different dimple aspect ratios 0.1, 0.2 and 0.3. ( $D = 130 \mu\text{m}$  and  $A_d = 16\%$  for all the samples).

effect might be directed with in the dimple inner surface with high dimple aspect ratios ( $a = 0.3$ ). So, it is presumed that enough hydrodynamic effect directed toward the counter surface was generated at a moderate aspect ratio of 0.2. A maximum frictional reduction of 69% was observed for the textured sample at a load of 130 N.

**4.4 Discussion on femtosecond laser assisted texturing**

Figure 12(a) shows a femtosecond pulsed laser textured ring sample with a dimple diameter of  $130 \mu\text{m}$  having an area density of 16% and aspect ratio of 0.2. To obtain dimples with the desired dimensions, the average laser power of 60 mW (laser energy  $60 \mu\text{J}$ ) and 4000 number of pulses were used. Laser texturing process parameters were selected based on preliminary trials. The corresponding dimple profile is shown in Fig. 12(b). Although at a high laser energy of around  $180 \mu\text{J}$ , a recast layer was observed, at a low laser energy of around  $60 \mu\text{J}$ , the recast was not observed with a high repetition rate of 1 kHz. Various research groups have reported on thermal accumulation effect with pulse repetition rates ranging from few hundred kHz to MHz order [21, 22]. As the repetition rate was comparatively lower and the laser ablation was performed at a low energy, influence of thermal accumulation in terms of melting, heat affected zone were not observed.

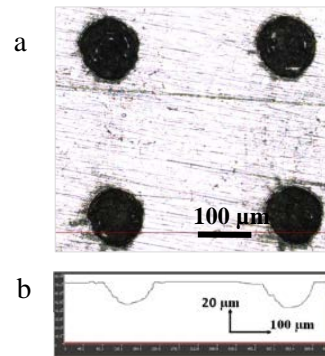


Fig. 12 (a) Femtosecond laser textured sample and (b) corresponding dimple profile ( $D = 130 \mu\text{m}$ ,  $A_d = 16\%$  and  $a = 0.2$ ).

Further cleaning process was not required as the ablated spot was clean and debris free. The tribometer results showed that friction coefficient observed with femtosecond pulsed laser textured sample was lower than that of nanosecond pulsed laser textured sample at a load of 130 N (Fig. 13). Changes in friction values at remaining less loads were not so significant. But at a high load of 130 N, a maximum of 76% reduction in friction compared to non-textured sample was observed with femtosecond pulsed laser textured sample.

The variations in friction coefficient in the case of both nanosecond and femtosecond pulsed laser textured samples of the same dimple dimension is attributed to the change in the magnitude of heat affected zone. The presence of heat affected zone was verified by measuring micro-hardness around the dimple circumference at various distances. For measuring hardness, a segment of ring sample with an arc length 6 mm was cut from a circular ring. Many dimples were generated both by nanosecond

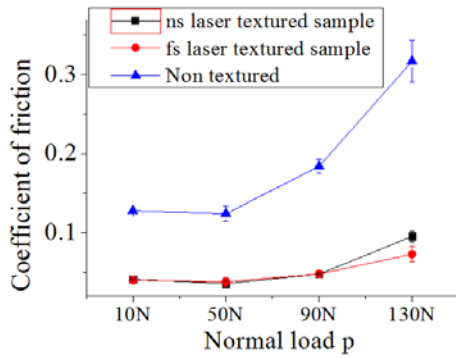


Fig. 13 Coefficient of friction graph for non-textured, nanosecond pulsed laser textured ( $D = 130 \mu\text{m}$ ,  $A_d = 16\%$  and  $a = 0.2$ ) and femtosecond pulsed laser textured ( $D = 130 \mu\text{m}$ ,  $A_d = 16\%$  and  $a = 0.2$ ) ring samples.

and femtosecond pulsed lasers and the hardness around dimples were measured. The microhardness results (Fig. 14) showed that there was an increase in hardness around the dimple ablated using nanosecond pulsed laser. The hardness of the moly-chrome material before laser ablation was measured to be around 941 HV. A maximum hardness of around 1106 HV was observed adjacent to the dimple circumference. The hardness value slowly decreased with the increase of distance from the dimple circumference and reached the hardness of moly-chrome material i.e., 941 HV at a distance of 90  $\mu\text{m}$  from dimple circumference. As the overall hardness of the textured ring surface increased after texturing with nanosecond pulsed laser, a high wear on the counter surface (liner) was noticed. The increase in wear induced more wear debris in the contact zone which in turn increased the friction coefficient. Whereas, with the femtosecond pulsed laser textured sample, the hardness around the dimple circumference almost remained unaffected. The wear on the counter sample was not so significant which resulted in less amount of wear debris in the contact zone. Hence, the friction coefficient was not altered by wear debris as in the case of nanosecond pulsed laser textured sample (Fig. 13). This verified the influence of thermal defects around the dimple circumference during the sliding test.

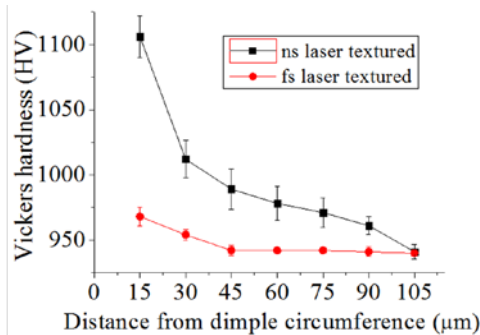


Fig. 14 Measurement of Vickers hardness as a function of distance from the dimple circumference for nanosecond and femtosecond pulsed laser textured ring sample ( $D = 130 \mu\text{m}$ ,  $A_d = 16\%$  and  $a = 0.2$  for both the samples).

### 5. Wear analysis

Wear analysis was performed on the liner surface after completing tribology test with all the piston ring samples. The roughness of the liner after testing with textured and non-textured samples was obtained and compared with the non-tested plain liner surface. The evaluated profile length for measuring surface roughness was 500  $\mu\text{m}$ . A reduction in surface roughness of the plateau honed pattern on the liner surface is the direct measurement of wear. Figures 15(a) to (d) shows the 3D surface morphology of the liner surface before and after testing with piston ring samples. The roughness  $R_a$  of the liner samples obtained from surface profiler is shown in Figs. 15(e-h). The liner was rough before testing because of the honed patterns (Fig. 15(a)). The liner roughness  $R_a$  before testing was measured to be 610 nm (Fig. 15(e)). The image of the liner surfaces

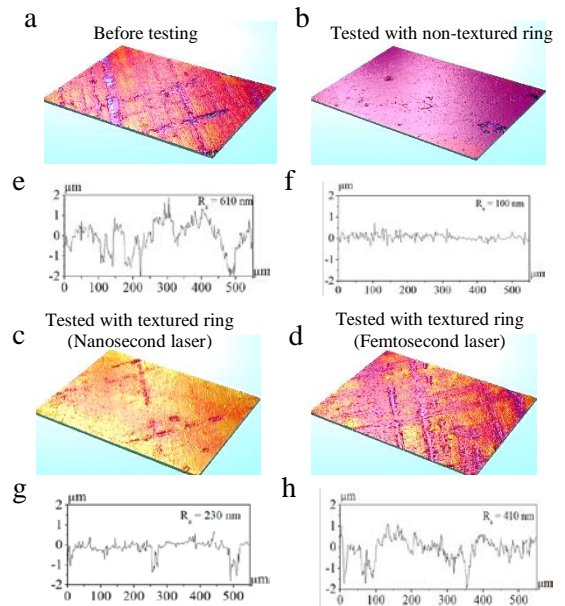


Fig. 15 Three-dimensional surface topography and corresponding roughness of liner surface at its dead centre (a) Before testing, (b) After testing with non-textured sample, (c) After testing with nanosecond pulsed laser textured sample ( $D = 130 \mu\text{m}$ ,  $A_d = 16\%$  and  $a = 0.2$ ) and (d) After testing with femtosecond pulsed laser textured sample ( $D = 130 \mu\text{m}$ ,  $A_d = 16\%$  and  $a = 0.2$ ).

after testing with non-textured, nanosecond pulsed laser textured ( $D = 130 \mu\text{m}$ ,  $A_d = 16\%$  and  $a = 0.2$ ) and femtosecond pulsed laser textured sample ( $D = 130 \mu\text{m}$ ,  $A_d = 16\%$  and  $a = 0.2$ ) are shown in Figs. 15(b-d). Their corresponding roughness  $R_a$  is shown in Figs. 15(f-h). The surface morphology revealed that the honed pattern was worn out completely after tested with non-textured ring sample. Whereas with textured ring sample, the honed pattern still existed after tribology testing though its roughness was minimized. This verifies that the textured piston ring sample improved the tribological properties between the ring and liner sliding pair.

The more wear on the liner surface is attributed to its lesser hardness (380 HV) compared to the hardness of moly-chrome coating (941 HV) located on the piston ring surface. Both abrasive and adhesive wear was observed on the liner surface. The presence of pits on the liner tested

with non-textured ring sample is a direct indication that scuffing took place. The abrasive wear was distinct by the loss of material from the liner surface by the rubbing action of harder piston ring material.

## 6. Conclusion

In the present work nanosecond pulsed Nd<sup>3+</sup>:YAG laser was used to generate textured surface in order to study the frictional characteristics between piston ring-liner contacts. Influence of loading conditions on the textured piston ring samples was experimentally investigated for the coefficient of friction. Based on the tribology studies, textured samples show comparatively lower values of coefficient of friction than that of non-textured samples. Dimple diameter of 40 µm and 80 µm showed minimum friction only at less loads. Whereas the dimple size of 130 µm showed a reduction in friction at a higher loading condition as well. High dimple area density of 38% proved to be detrimental and the friction was high compared to all the samples.

The optimum area density to minimize friction was maintained at 16% at almost all the loads. Studies on the influence of aspect ratio revealed that an aspect ratio of 0.2 showed a minimized friction. A maximum of 69% friction reduction was observed with nanosecond pulsed laser textured sample. A slight improvement in friction reduction (76%) was observed with femtosecond pulsed laser textured sample. The wear was quantified by the reduction of roughness on the liner surface. The wear on the liner surface tested with the non-textured sample was high compared to that of the textured sample. The liner surface was almost intact when tested with femtosecond pulsed laser textured sample.

## Acknowledgements

The authors are grateful to MEMS lab and SEM lab for the technical supports. The authors would like to thank Dr. Anil of VIT, Dr. Mahadevan from India pistons limited and Dr. Sebastian of IIT Madras for their continuous support. The research work is partially supported by the DST-AMT Program (DST/TSG/AMT/2015/353).

## Reference

- [1] A. Zavos and P. Nikolakopoulos: Tribol. Ind., 37, (2015) 1.
- [2] I. Etsion and E. Sher: Tribol. Int., 42, (2009) 542.
- [3] B.G. Rosén, B. Nilsson, T.R. Thomas, D. Wiklund, L. Xiao, The XI. International Colloquium on Surfaces, Chemnitz, Germany (2004).
- [4] Y. Wan and D.S. Xiong: J. Mater. Process. Technol., 197, (2008) 96.
- [5] I. Etsion: Friction, 1, (2013) 195.
- [6] Y Zhang, X Zhang, T Wu, and Y. B. Xie: Ind Lubr Tribol., 68, (2016) 158.
- [7] I. Etsion, Y. Kligerman, and A. Shinkarenko: Trans. ASME, J. Tribol., 123, (2005) 632.
- [8] C. Gu, X. Meng, Y. Xie and P. Li: Proceedings of the Institution of Mechanical Engineers, Part J: J. Eng. Tribol., 230, (2016) 452.
- [9] M. Wakuda, Y. Yamauchi, S. Kanzaki and Y. Yasuda: Wear, 254, (2003) 356.
- [10] D. Yan, N. Qu, H. Li and X. Wang: Tribol. T., 53, (2010) 703.
- [11] H. Zhang, M. Hua, G.n. Dong, D.y. Zhang and K.S. Chin: Tribol. Int., 93, (2016) 583.
- [12] M. Wakuda, Y. Yamauchi, S. Kanzaki and Y. Yasuda: Wear, 254, (2003) 356.
- [13] Y. Zhou, H. Zhu, W. Tang, C. Ma and W. Zhang: Tribol. Int., 52, (2012) 1.
- [14] B. Kim, Y. H. Chae and H. S. Choi: Tribol. Int., 70, (2014) 128

- [15] W. Tang, Y. Zhou, H. Zhu and H. Yang: Appl. Surf. Sci., 273, (2013) 199.
- [16] D. Braun, C. Greiner, J. Schneider and P. Gumbsch: Tribol. Int., 77, (2014) 142.
- [17] W. Grabon, W. Koszela, P. Pawlus and S. Ochwat: Tribol. Int., 61, (2013) 102.
- [18] A. Kovalchenko, O. Ajayi, A. Erdemir, G. Fenske and I. Etsion: Tribol. Int., 38, (2005) 219.
- [19] V. Ezhilmaran, L. Vijayaraghavan, N. Vasa, S. Ganesan and N. Cherian: J. Laser Micro/Nanoeng., 11, (2016) 179.
- [20] H. Yu, W. Huang, and X. Wang: Lubr. Sci., 25, (2013) 67.
- [21] A. Ancona, S. Döring, C. Jauregui, F. Röser, J. Limpert, S. Nolte and A. Tünnermann: Opt Lett., 34, (2009) 3304.
- [22] F. Di Niso, C. Gaudiuso, T. Sibillano, F. P. Mezzapesa, A. Ancona, and P. M. Lugarà: Phys. Procedia, 41, (2013) 698.

(Received: June 5, 2017, Accepted: September 30, 2017)